

Nanomagnetite-supported molybdenum oxide (nanocat-Fe-Mo): an efficient green catalyst for multicomponent synthesis of amidoalkyl naphthols

Swapnil R. Bankar¹  · Sharad N. Shelke¹

Received: 29 November 2017 / Accepted: 2 February 2018
© Springer Science+Business Media B.V., part of Springer Nature 2018

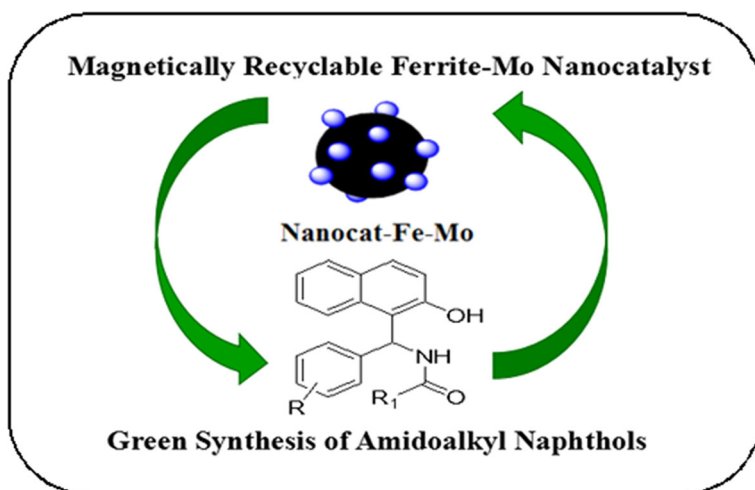
Abstract Magnetite (Fe_3O_4)-supported molybdenum oxide (MoO_3) was synthesized from simple starting precursors in aqueous medium. The synthesized nanocat-Fe-Mo was analyzed using several techniques such as X-ray diffraction (XRD) analysis, X-ray photoelectron spectroscopy (XPS), scanning electron microscopy (SEM), transmission electron microscopy (TEM), and vibrating-sample magnetometry (VSM). The catalytic activity of the synthesized nanocat-Fe-Mo was studied in a benign one-pot multicomponent transformation for synthesis of amidoalkyl naphthol derivatives under solvent-free condition using both conventional and microwave irradiation methods. Nanocat-Fe-Mo was found to be highly active and could be reused seven times without notable loss in catalytic activity. The proposed method offers advantages such as good reaction yield (80–95%), short process time, simple workup, and recycling of the catalyst, representing important green chemistry principles.

Electronic supplementary material The online version of this article (<https://doi.org/10.1007/s11164-018-3321-4>) contains supplementary material, which is available to authorized users.

✉ Sharad N. Shelke
snsшелke@yahoo.co.in

¹ P. G. and Research Centre, Department of Chemistry, S.S.G.M. College, Kopergaon, Ahmednagar, MS 423601, India

Graphical Abstract



Keywords MNPs · Nanocat-Fe-Mo · Multicomponent reaction · Amidoalkyl naphthols · Benign media · Green transformation

List of symbols

Ar	Aryl
CCD	Charge coupled device
DMF	Dimethyl formamide
DMSO	Dimethylsulfoxide
EDS	Energy dispersive spectroscopy
Fe-Mo	Ferrite-molybdenum
FT-IR	Fourier-transform infrared
FWHM	Full width at half maximum
HIV	Human immunodeficiency virus
ICP-AES	Inductively coupled plasma-atomic emission spectroscopy
LFD	Large field detector
MNPs	Magnetic nanoparticles
MP	Melting point
MW	Microwave
NMR	Nuclear magnetic resonance
NP	Nanoparticle
Ph	Phenyl
ppm	Parts per million
RBF	Round-bottomed flask
RF	Radiofrequency
RT	Room temperature
SEM	Scanning electron microscopy

TEM	Transmission electron microscopy
TLC	Thin-layer chromatography
TMS	Tetramethylsilane
UV	Ultraviolet
VSM	Vibrating-sample magnetometry
XRD	X-ray diffraction

Introduction

Working towards sustainability, researchers have made significant advances in organic transformations by using nanoparticle materials, attracting great attention in areas such as drug discovery [1, 2], electronic field devices [3], as well as heterogeneous catalysis [4, 5]. Over the past few decades, ecofriendly heterogeneous catalysts have played a vital role in organic transformations [6]. Application of NPs in heterogeneous catalysis has become an important focus, including nanosupported metal catalysts, solid-supported inert platforms such as silica, and iron oxides in biological transformations. Iron-oxide-based NPs have been widely used as an important support for functionalization of metals, organocatalysts, chiral catalysts, and *N*-heterocyclic carbenes [7].

During the last decade, nanocatalysts, especially supported on noble metals such as Au, Ru, Mo, Pt, and Pd, have introduced a fertile area of selective organic methodologies as well as catalytic reactions [8, 9]. Immobilization of molybdenum on solid supports has mainly been applied in a number of important organic reactions, including A3 coupling, hydrogenation, and hydration, as well as oxidation of benzyl alcohol [10–12]. In such organic transformations, supported catalysts offer the advantage of bypassing problems related to inefficient heating and use of activation methods such as mechanochemical grinding or ultrasonic and microwave (MW) irradiation for such syntheses [13–17]. Among these processes for rapid organic synthesis using faster and cleaner approaches, MW heating has also emerged as an important energy source [18–21]. In addition, solvent-free approaches for chemical reactions also represent a growing trend from the point of view of green chemistry with respect to future resources and chemical waste [22].

In recent years, multicomponent reactions have attracted particular attention from researchers, being considered a special field of combinatorial chemistry because of their capacity for synthesis of complex compounds in one pot [23]. MCRs offer key features of green chemistry, since many reagents are added in a single step to form a novel molecule without any intermediates. The advantages of such reactions include atom economy, reduced processing time, simple workup method, as well as enabling environmentally friendly synthesis [24–26].

Literature survey reveals that 1-amidoalkyl-2-naphthols and their derivatives including, e.g., [1,3]oxazine nucleus represent important compounds for synthesis of many natural products, antibiotics, nucleosides, and human immunodeficiency virus (HIV) protease inhibitors such as ritonavir and lopinavir [27, 28]. By amide

hydrolysis reaction, 1-amidoalkyl-2-naphthols can be converted to 1-aminomethyl-2-naphthol derivatives, which have important bioactivity and exhibit bradycardia and depressor effects in humans [29, 30].

Research has been carried out on synthesis of amidoalkyl naphthols by combination of aldehydes, 2-naphthols, and amides via various multicomponent pathways, e.g., in presence of catalysts such as iodine [31, 32], ionic liquids [33], montmorillonite clay, MgSO_4 , ZnO nanoparticles, $\text{HClO}_4\text{-SiO}_2$, various Lewis and Brønsted acids [34–39], and $\text{K}_5\text{CoW}_{12}\text{O}_{40}\cdot 3\text{H}_2\text{O}$ [39]. However, some of these reported methods suffer from certain disadvantages such as use of harmful solvents, longer reaction time, expensive catalyst, low yield, and harsh reaction conditions such as high temperature. In view of these drawbacks of previous methods and to attain sustainability, it is important to develop ecofriendly clean procedures with good catalytic activity for preparation of 1-amidoalkyl-2-naphthols.

Considering these problems, we present herein a simple, green, sustainable protocol for one-pot MCR of amidoalkyl naphthols using a highly active magnetite-supported molybdenum oxide nanocatalyst. Our researcher group previously reported [10] Mo-functionalized magnetite, active in oxidation and reduction processes, as well as MCR and coupling chemistries. The advantages of using such Mo-based Fe catalysts include recyclability and facile handling [10]. MNPs were prepared by simple wet impregnation methods in benign medium. In continuation of our research on development of greener techniques and novel methodologies [40], we have developed here a novel and simple scheme for functionalization of ferrite MNPs with molybdenum oxide as Lewis acid site for one-pot MCRs. To the best of the authors' knowledge and as revealed by literature survey, no earlier reports are available on use of such Mo-based magnetite catalysts for synthesis of amidoalkyl naphthols.

Experimental

Resources and reagents

For the current investigation, all commercial chemicals were obtained from Sigma-Aldrich and used as received. All reactions were carried out using a laboratory microwave oven (RAGA'S Scientific Microwave System-700 W). All reported melting points were determined using a model KI-11 (MP-D) melting point apparatus (Kumar Sales Corporation, Mumbai, India) and are uncorrected. Reaction progress was monitored with the help of preparative TLC on precoated silica gel glass plates (Kieselgel 60 mit Fluoreszens-Indicator UV- 254, E. Merck, Germany). Spots were visualized using ultraviolet (UV) light.

Characterization techniques

XRD analysis was carried out on the newly synthesized Mo-ferrite nanocatalyst. The X-ray powder diffraction pattern was obtained using a conventional powder diffractometer (MiniFlexTM II benchtop X-ray diffractometer, Rigaku) with Cu K_α

radiation X-ray tube (30 kV/15 mA) operating in Bragg–Brentano (θ – 2θ) geometry. Samples were prepared by grinding when needed and compressed in the sample holder with a flat glass. The sample area in the sample holder was about 2 cm².

XPS measurements were performed on a VSW XPS system with class 100 energy analyzer, being part of an experimental setup assembled for surface investigation [41]. Spectra were measured in fixed analyzer transmission mode with FAT 22 mode (energy step 0.1 eV, acquisition time 24 s). Nanoparticle powder was prepared for XPS by pressing on indium (In) plate as matrix to provide mechanical support and reduce charging problems. For energy axis calibration, Ag (110) and polycrystalline Au samples (previously cleaned by ion sputtering) were used.

TEM experiments were performed on a Hitachi H8100 microscope using a ThermoNoran light-elements energy-dispersive X-ray spectroscopy (EDS) detector and charge-coupled device (CCD) camera for image acquisition. The nanocat-Fe-Mo fine powder was placed on a carbon stub, and images were recorded at 5–15 kV using a large-field detector (LFD) under low vacuum. SEM images were acquired using a JEOL JSM7001F FEG-SEM. Elemental analysis was performed using a light-elements EDS detector from Oxford. Nanocat-Fe₃O₄-MoO₃ powder was spread on double-sided carbon tape and analyzed at acceleration voltage of 25 kV.

Elemental analysis was carried out by inductively coupled plasma-atomic emission spectrometry (ICP-AES, Ultima; Horiba Jobin–Yvon, France) equipped with a 40.68 MHz radiofrequency (RF) generator, Czerny–Turner monochromator with 1.00 m (sequential), AS500 autosampler, and concomitant metals analyzer (CMA). The magnetic properties of the Fe₃O₄ materials were analyzed by vibrating-sample magnetometry (VSM, Lakeshore 7404) at room temperature. FT-IR spectra were scanned on a PerkinElmer Spectrum version 10.4.2. NMR spectra were recorded on a Bruker 300 MHz (¹H NMR) and 75 MHz (¹³C NMR) instrument with CDCl₃ or DMSO as solvent and TMS as internal standard; chemical shifts (δ) are stated in ppm, and coupling constants (J) in Hertz. Signal splitting is denoted by *s* (singlet), *d* (doublet), *t* (triplet), *dd* (double doublet), and *m* (multiplet).

Preparation of ferrite MNPs [40–42]

FeCl₃·6H₂O (5.4 g) and urea (3.6 g) were dissolved in water (200 mL) for 2 h at 85–90 °C. The solution color became brown. To this brown reaction mixture cooled at room temperature was added FeSO₄·7H₂O (2.8 g), and then NaOH (0.1 M) until the pH became 10. In this case, the molar ratio of Fe(III) to Fe(II) is nearly 2.00. The resultant hydroxide was treated by ultrasonication in sealed flasks at 30–35 °C for 30 min. After aging for 5 h, the resulting black powder (Fe₃O₄) was purified and dried under vacuum.

Preparation of nanocat-Fe-Mo MNPs [10–12]

Ferrite MNPs, Fe₃O₄ (2 g), and ammonium molybdate (NH₄)₆Mo₇O₂₄·4H₂O (0.147 mg to get 1–2% Mo) were stirred at room temperature in aqueous medium (50 mL) for 1 h. After impregnation, the suspension pH was adjusted to 12 by adding sodium hydroxide (1.0 M), followed by stirring for 20 h. The resultant solid

was washed with distilled water (five times, 10 mL). The obtained metal precursors were reduced by adding 0.2 M NaBH₄ water solution dropwise under gentle stirring in ice–water bath for 30 min until no bubbles were obtained in the solution. The resulting nanocat-Fe-Mo MNPs were kept under ultrasonication for 10 min then washed with distilled water and subsequently with ethanol and dried under vacuum at 60 °C for 24 h. The Mo content in the nanocatalyst was determined to be 0.42 wt% by ICP-AES analysis.

One-pot synthesis of amidoalkyl naphthols using nanocat-Fe-Mo

For synthesis of amidoalkyl naphthol analogs, a combination of 2-naphthol (10 mmol), substituted aromatic aldehyde (10 mmol), urea (12 mmol), and nanocat-Fe-Mo (10 mol%) was added. The reaction was performed conventionally at 120 °C for 30 min under solvent-free conditions. The same reaction mixture was also carried out in the microwave oven at 350 W in benign medium, for comparison. The microwave oven was adjusted to boost the internal reaction temperature to 120 °C within 1 min, and then continue with appropriate irradiation (0–700 W) at the same temperature, for the suitable time. Reaction monitoring was carried out with the help of TLC. It was observed that, compared with the conventional oil bath heating process, the nonconventional MW technique was superior and clean.

After completion, the reaction content was cooled to room temperature, then the solid mixture was dissolved in boiling ethanol and stirred for 2 min. The solution was then filtered by magnetic decantation technique. The solid obtained on cooling the solution to room temperature was purified by column chromatography technique on silica bed using *n*-hexane and ethyl acetate as eluent, and the final solid obtained

Table 1 Ferrite-Mo-catalyzed synthesis of amidoalkyl naphthol analogs (**4a–l**): yields and melting points

4	R	R ₁	M.p. (°C)	Method A Time (min)/yield (%)	Method B Time (min)/yield (%)
4a	H	CH ₃	240	3/94	30/94
4b	H	NH ₂	170	3/92	40/91
4c	4-CH ₃	CH ₃	216	3.5/95	35/86
4d	4-CH ₃	NH ₂	172	4/89	30/93
4e	4-Cl	CH ₃	228	4/92	30/94
4f	4-Cl	NH ₂	165	4/86	35/86
4g	4-OCH ₃	CH ₃	210	5/92	45/81
4h	4-OCH ₃	NH ₂	190	3/90	40/92
4i	4-Br	CH ₃	248	4/92	30/90
4j	4-Br	NH ₂	172	4/87	35/86
4k	4-NO ₂	CH ₃	224	4/90	35/90
4l	4-NO ₂	NH ₂	178	4/93	30/80

Method A, microwave technique; method B, oil bath

was analyzed by melting point measurements and TLC R_f values. Catalyst was recovered by evaporation of organic solvents under reduced pressure and drying well using vacuum. Nanocat-Fe-Mo was used again without loss of activity. Different analogs were obtained by following the same experimental process. The compounds synthesized using the above-described procedure are summarized in Table 1 together with their characterization data. All known compounds were reported earlier in literature and were characterized by comparison with NMR spectra of authentic samples.

The method using the presented Fe-Mo catalyst was also compared with other inorganic and organic catalysts reported in literature for synthesis of amidoalkyl naphthol derivatives (Table 2), clearly showing that the present nanocat-Fe-Mo catalyst was more efficient compared with reported procedures.

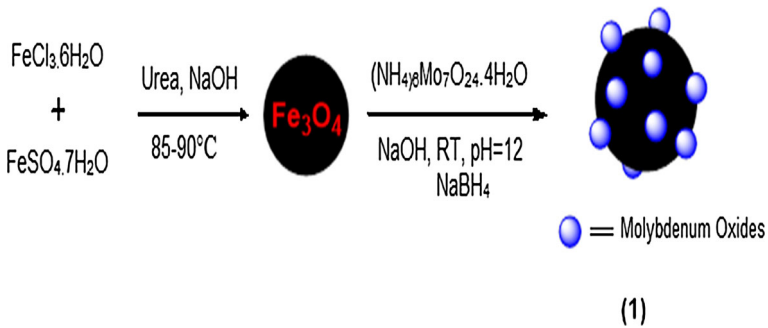
Results and discussion

Magnetic nanocat-Fe-Mo characterization

Magnetically recyclable nanocat-Fe-Mo was prepared from ferrite NPs and ammonium molybdate by simple wet impregnation method in benign medium (Scheme 1) and characterized using various techniques including X-ray diffraction (XRD) analysis, inductively coupled plasma-atomic emission spectroscopy (ICP-

Table 2 Comparison of synthesis of amidoalkyl naphthol using nanocat Fe-Mo with other catalysts reported in literature

No.	Catalyst	Conditions	Yield (%)	References
1	Ce(SO ₄) ₂	CH ₃ CN reflux, 36 h	66–78	[31]
2	Iodine	Solvent free, 125 °C, 5 h	71–84	[32]
3	Montmorillonite K10	Solvent free, 125 °C, 1.5 h	70–78	[37]
4	MgSO ₄	Solvent free, 100 °C, 1 h	72–90	[36]
5	ZnO NPs	Solvent free, (a) 130 °C, 30 min (b) MW, 6 min	81–94	[34]
6	Imidazolium salt	Solvent free, 120 °C, 40 min	81–95	[46]
7	H ₄ SiW ₁₂ O ₄₀	Solvent free, 110 °C	78–94	[47]
7	Trityl chloride	Room temp., 1–4 h	83–94	[48]
8	<i>p</i> -TSA	Solvent free, 125 °C, 4–8 h	83–93	[49]
9	MNPs-PhSO ₃ H	Solvent free, 120 °C, 40 min	81–94	[50]
10	MSNs-HPZ-SO ₃ H	Solvent free, 120 °C, 60 min	75–94	[51]
11	Ferrite-Mo	Solvent free, 120 °C, 30 min	84–96	Present work
12	Ferrite-Mo	Solvent free, MW, 3 min	86–94	Present work



Scheme 1 Synthesis of nanocat-Fe-Mo (1)

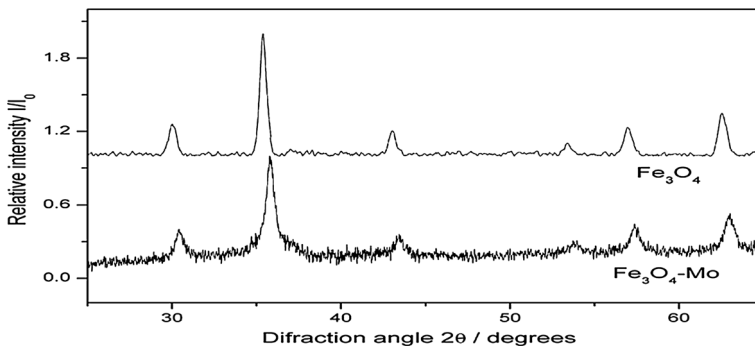


Fig. 1 XRD pattern of nano-Fe-Mo catalyst with reference to magnetite

AES), X-ray photoelectron microscopy (XPS), transmission electron microscopy (TEM), field-emission-gun scanning electron microscopy with energy-dispersive spectrometry (FEG-SEM-EDS), and vibrating-sample magnetometry (VSM). The Mo content in the nanocatalyst was determined to be 0.40 wt% by ICP-AES analysis.

The crystallite size of the Fe-Mo MNPs was determined using the Debye-Scherrer equation. The XRD spectra of the ferrite and nanocat-Fe-Mo nanoparticles (Fig. 1) showed that the crystallite size of the nanocat-Fe-Mo MNPs was 30.1 nm, similar to the TEM result indicating size distribution between 20 and 40 nm. Due to the low percentage (0.42 wt%) of Mo, no diffraction lines corresponding to the Mo oxides observed by XPS method could be detected by XRD.

To confirm the oxidation state and nature of the Mo species in the nanocatalyst, the nanocat magnetite-Mo was analyzed by X-ray photoelectron spectroscopy (XPS). The surface composition of the MNP powder was determined from the intensities of the characteristic XPS peaks of C, O, Fe, and Mo, viz. C 1s, O 1s, Fe 2p, and Mo 3d, respectively. In the final nanocatalyst, oxygen appeared to be the most abundant element (51.2%), followed by carbon (34.1%), iron (10.3%), and molybdenum (0.4%). The Mo content obtained from XPS was found to be in agreement with that measured by ICP-AES technique, revealing that the Mo was

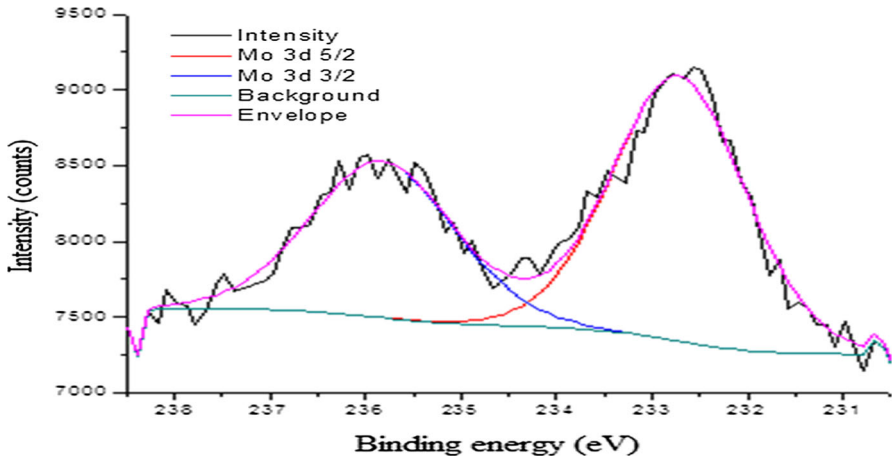


Fig. 2 Mo 3d XPS spectrum of Mo-Fe₃O₄ nanocatalyst

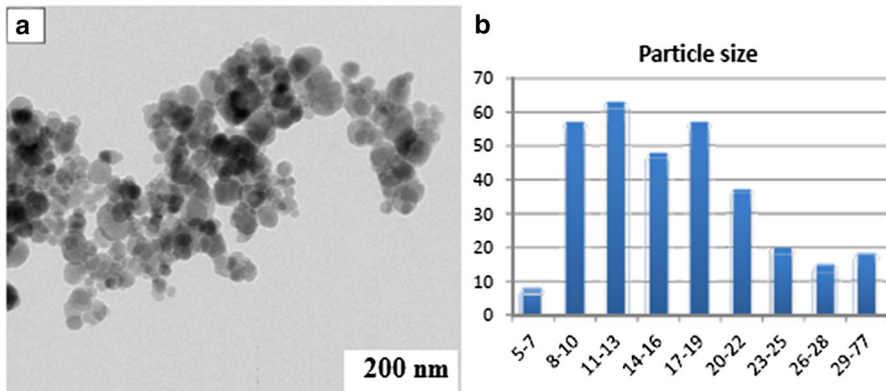


Fig. 3 a TEM image of nanocat-Fe-Mo at 200 nm. b Histogram of nanocat-Fe-Mo

present on the surface of the nanoferrite in the final nanocatalyst. The main characteristic peaks of molybdenum (Mo 3d) are shown in Fig. 2. The two peaks ($3d_{5/2}$ and $3d_{3/2}$) have intensity ratio of 62:38 (close to the theoretical ratio of 60:40), with full-width at half-maximum (FWHM) of about 1.68 eV. The $3d_{5/2}$ line appeared at 232.7 eV, perfectly matching with the MoO₃ state in literature [43, 44].

TEM of nanocat-ferrite-Mo (Fig. 3) revealed that the synthesized MNPs exhibited uniform size with somewhat spherical morphology. The diameter of the NPs ranged from 20 to 40 nm (average 20 nm), consistent with the XRD results.

FEG-SEM analysis of the nanomagnetite-Mo sample was carried out at acceleration voltage of 25 kV, revealing nanoparticles of uniform size and somewhat spherical morphology with woolly cloud-like clusters (Fig. 4).

After characterization, the catalytic activity of nanocat-Fe-Mo was investigated in a series of reactions to confirm its versatility due to the contained Mo.

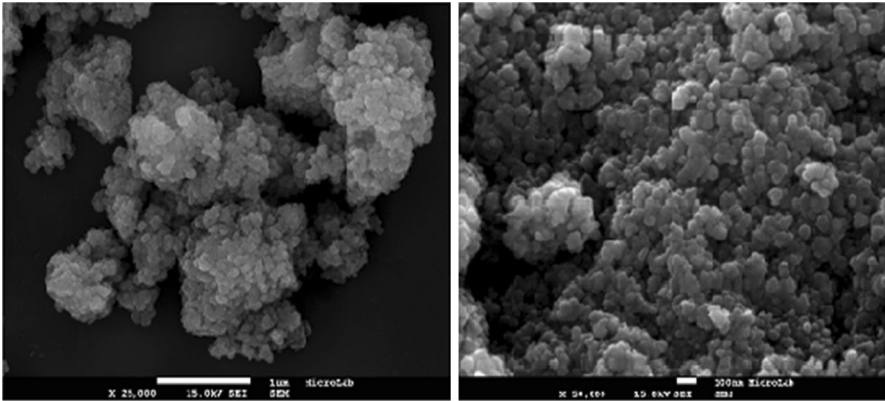


Fig. 4 SEM images of nanocat-Fe-Mo nanoparticles

Fig. 5 SEM images of recovered catalyst after seventh cycle

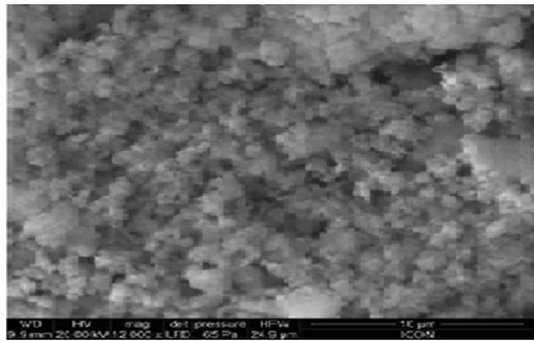
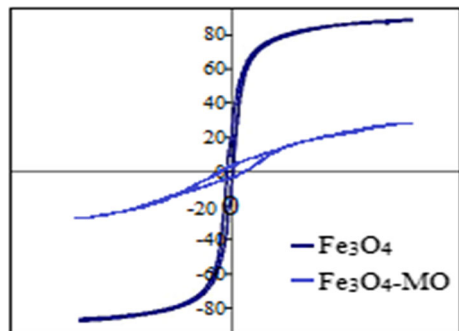


Fig. 6 VSM curve of synthesized Fe_3O_4 and Fe-Mo-coated nanomaterial



After the seventh cycle, recovered catalyst was characterized by SEM, showing almost the same results as for freshly synthesized catalyst with no significant changes (Fig. 5). Meanwhile, it is important to stress that reactions carried out using nonfunctionalized ferrite (without Mo) delivered no/low yield in the studied reactions.

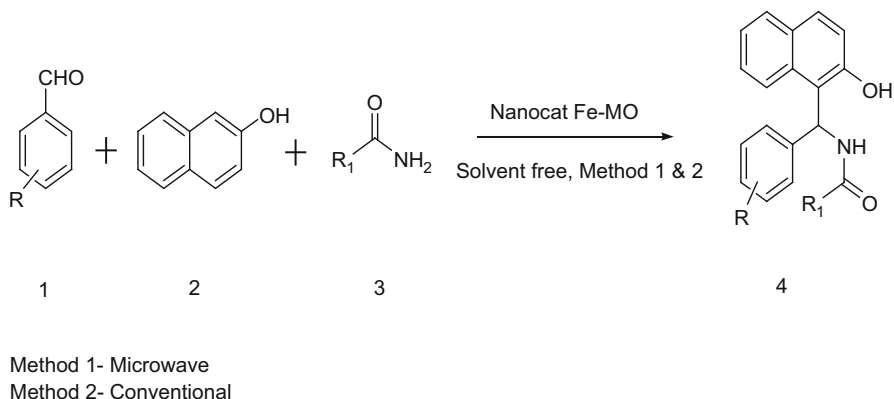
To study the magnetic properties of the synthesized ferrite nanomaterial, the magnetization curve of Fe_3O_4 material obtained by VSM at room temperature is shown in Fig. 6. The saturation magnetization of the Fe_3O_4 nanoparticles was found to be 88.69 emu g^{-1} , not far from the actual magnetization of Fe_3O_4 of 92 emu g^{-1} [45]. After application of molybdenum on the ferrite, the magnetic moment of the sample dropped to 22.46 emu g^{-1} , clearly confirming the coating of molybdenum on the ferrite material.

Nanocat-Fe-Mo-catalyzed multicomponent synthesis of amidoalkyl naphthols

To confirm the efficacy and scope of the synthesized and characterized nanocat $\text{Fe}_3\text{O}_4\text{-Mo}$ in MCRs, aromatic aldehydes and amides were subjected to one-pot condensation with 2-naphthol in presence of catalytic amount of nanocat-Fe-Mo to obtain 1-amidoalkyl 2-naphthol analogs. All reactions proceeded smoothly when using the conventional method (120°C , 30 min) or under microwave irradiation at 350 W for 3–6 min. The reaction progressed well under MW in solvent-free conditions and benign medium with good product yield (Scheme 2).

Another possibility is quantitative formation of 14-aryl-14*H*-dibenzo[*a,j*]xanthenes when β -naphthol is used with aldehyde in 2:1 molar ratio. However, use of 1:1 mol ratio of β -naphthol and aldehyde with urea in presence of nanocat-Fe-Mo exclusively resulted in amidoalkyl naphthols. To optimize the reaction conditions, we selected as model reaction that of aromatic aldehyde with 2-naphthol, urea, and nanocat-Fe-Mo under solvent-free condition at $120\text{--}130^\circ\text{C}$ (Table 3).

In further study, condensation of β -naphthol, aromatic aldehyde, and urea was examined in presence of different quantities of nanocat-Fe-Mo at reaction temperature (Table 4). As indicated in Table 4, reasonable results were obtained when the reaction was performed using 10 mol% nanocat-Fe-Mo (entry 2), with no improvement observed on increasing the amount of nanocatalyst (entries 3, 4).



Scheme 2 Nanocat-Fe-Mo-catalyzed synthesis of amidoalkyl naphthols under solvent-free condition

Table 3 Optimization of reaction condition^a

S. no.	Catalyst	Solvent	Time (min)	Temp.	Yield ^b
1	No catalyst	–	1440 min	RT	NR
2	No catalyst	–	1440 min	100 °C	Trace
3	Nanocat-Fe-Mo	–	60 min	RT	Trace
4	Nanocat-Fe-Mo	–	1440 min	RT	35
5	Nanocat-Fe-Mo	–	30 min	120 °C	91
6	Nanocat-Fe-Mo	–	3–6 min (MW)	120 °C	94
7	Nanocat-Fe-Mo	H ₂ O	30–40 min	120 °C	80
8	Nanocat-Fe-Mo	EtOH	120 min	120 °C	78

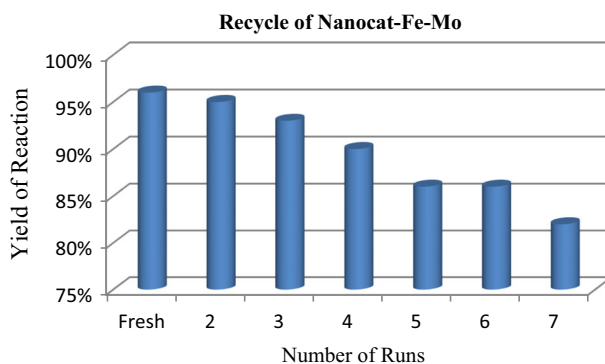
^aReaction condition: 2-naphthol (10 mmol), aromatic aldehyde (10 mmol), urea (12 mmol), nanocat-Fe-Mo (10 mol%), temperature 120–130 °C, heating in sealed RBF; NR (no reaction)

^bIsolated yield of pure product

Table 4 Effect of amount of catalyst on reaction yield

Entry	Catalyst amount (mol%)	Time (h)	Yield ^a (%)
1	5	3	80
2	10	1	94
3	15	1	94
4	20	1	94

^aIsolated yield

**Fig. 7** Reusability of nanocat-Fe₃O₄-MoO₃

In addition to the applicability and advantages of the synthesized nanocat-Fe-Mo in the studied reaction, its stability was also checked by recycling. After each cycle, the catalyst was separated magnetically, washed with ethanol, and finally dried at 60 °C under vacuum to remove residual solvent. The nanocat was utilized for other analogs of the same series under the same reaction condition. The results after various cycles with reaction yield are shown in Fig. 7. The catalyst could be used up to seven times without considerable loss of its initial catalytic activity. In absence of

Table 5 Solvent effect on reaction using nanocat-Fe-Mo

Entry	Solvent ^a	Condition	Yield ^b (%)
1	EtOH	Reflux, 2 h	78
2	DMF	Reflux, 3 h	62
3	<i>n</i> -Hexane	Reflux, 3 h	58
4	Solvent free	120 °C, 30 min	96

^a1 mL solvent^bIsolated yield**Table 6** Effect of temperature on reaction yield

Entry	Reaction temperature (°C)	Reaction yield (%)
1	70	57
2	100	81
3	120	94
4	150	91

nanocat-Fe-Mo, no fruitful results were obtained under the same reaction conditions even after 12 h.

To compare the effect of solutions versus the solvent-free condition, we also carried out the reaction in both presence and absence of solvents such as EtOH, dimethylformamide (DMF), and *n*-hexane. Nearly all reactions were less efficient in presence than absence of solvent, in terms of both reaction time and yield (Table 5).

To study the effect of temperature, the three-component reaction was carried out at four different temperatures of 70, 100, 120, and 150 °C. Notably, the best results were obtained at 120 °C (Table 6, entry 3). With further increase of the temperature, no considerable increase in yield was observed (Table 6, entry 4). Therefore, all other reactions were carried out at 120 °C.

Initially, for comparison with the reactions performed using MNPs (Tables 1, 2), compounds **4a–h** were also obtained using the conventional, refluxing method, obtaining low yields (Tables 1, 2). In contrast, when carrying out the same reactions in presence of MNPs by the microwave irradiation method, very clean products were obtained in appreciably higher yield. All experiments were carried out three times to confirm the reliability of the results.

Spectral data of some synthesized compounds

Compound **4b**: ¹H NMR (300 MHz CDCl₃, δ, ppm): 6.08 (2H, bs, –NH₂), 7.17–7.18 (1H, *d*, –ArOH), 7.19–7.49 (7H, *m*, –ArH), 7.62–7.64 (4H, *m*, –ArH), 7.73–7.78 (1H, *t*, –ArH), 9.25 (1H, *s*, –CONH).

¹³C NMR (75 MHz, CDCl₃): 46.31, 116.56, 119.89, 122.97, 127.67, 128.23, 128.59, 128.96, 129.05, 129.38, 131.44, 132.84, 134.32, 138.30, 149.01, 161.56.

Compound **4g**: ¹H NMR (300 MHz CDCl₃, δ, ppm): 2.05 (3H, *s*, –COCH₃), 3.42 (3H, *s*, –OCH₃), 5.10 (1H, bs, –CH), 6.00 (1H, bs, –Ar-OH), 7.39–7.72 (10H, *m*, –ArH), 9.05 (1H, bs, –CONH).

^{13}C NMR (75 MHz, CDCl_3): 32.07, 40.85, 50.76, 114.82, 115.10, 115.27, 118.83, 124.91, 126.10, 127.39, 129.25, 130.67, 130.83, 130.93, 139.94, 151.33, 160.98, 161.91, 164.24.

Conclusions

The present work provides a simple approach for one-pot MCR for synthesis of amidoalkyl naphthols in good yield using magnetically reusable nanocat-Fe-Mo as catalyst. This method offers various benefits such as atom economy and use of less hazardous chemicals in an economic and environmentally friendly process. Moreover, use of the microwave irradiation technique for direct heating of the reaction mixture and the solvent-free mild condition continue our efforts to identify green routes following sustainable methodologies.

Acknowledgements S.R.B. gratefully thanks the BCUD, Savitribai Phule Pune University, Pune for granting research stipend. The authors are grateful to the Director of SAIF, Panjab University (Chandigarh, India) for spectral analysis. S.R.B. thanks Dr. M. B. Gawande for constant inspiration. We also acknowledge the HOD and Principal, S.S.G.M. College, Kopargaon, Ahmednagar (MH) for providing research facilities.

Compliance with ethical standards

Conflict of interest The authors declare they have no competing financial interests.

References

1. G. Spada, E. Gavini, M. Cossu, G. Rassu, P. Giunchedi, *Nanotechnology* **23**(9), 095101 (2012)
2. T.L. Doane, C. Burda, *Chem. Soc. Rev.* **41**, 2885 (2012)
3. V. Berry, R.F. Saraf, *Angew. Chem. Int. Ed.* **44**, 6668 (2005)
4. A. Schatz, T.R. Long, R.N. Grass, W.J. Stark, P.R. Hanson, O. Reiser, *Adv. Funct. Mater.* **20**, 4323 (2010)
5. M.B. Gawande, S.N. Shelke, A.K. Rathi, P.S. Branco, R.K. Pandey, *Appl. Organometal. Chem.* **26**, 395 (2012)
6. A. Baiker, *Chem. Rev.* **99**(2), 453 (1999)
7. M.B. Gawande, P.S. Branco, R.S. Varma, *Chem. Soc. Rev.* **42**, 3371 (2013)
8. B.R. Vaddula, A. Saha, R.S. Varma, *Green Chem.* **14**(8), 2133 (2012)
9. S. Sa, M.B. Gawande, A. Velhinho, J.P. Veiga, R.S. Varma, P.S. Branco, *Green Chem.* **16**, 3494 (2014)
10. M.B. Gawande, P.S. Branco, I.D. Nogueira, N. Bundaleski, O. Teodoro, R. Luque, *Green Chem.* **15**(3), 682 (2013)
11. K. Routray, W. Zhou, C.J. Kiely, I.E. Wachs, *J. Catal.* **275**, 84 (2010)
12. R. Luque, B. Baruwati, R.S. Varma, *Green Chem.* **12**, 1540 (2010)
13. M.B. Gawande, S.N. Shelke, R. Zboril, R.S. Varma, *Acc. Chem. Res.* **47**(4), 1338 (2014)
14. V. Polshettiwar, R.S. Varma, *Chem. Soc. Rev.* **37**, 1546 (2008)
15. V. Polshettiwar, R.S. Varma, *Acc. Chem. Res.* **41**, 629 (2008)
16. V.V. Nambodiri, R.S. Varma, *Org. Lett.* **4**, 3161 (2002)
17. R.S. Varma, *Appl. Sci.* **4**, 493 (2014)
18. C.R. Strauss, R.S. Varma, *Microwaves in Green and Sustainable Chemistry*, vol. 266 (Springer, Heidelberg, 2006), p. 199

19. A. Bruckmann, A. Krebs, C. Bolm, *Green Chem.* **10**, 1131 (2008)
20. R.S. Varma, *ACS Sustain. Chem. Eng.* **4**, 5866 (2016)
21. A. Hasaninejad, A. Zare, M. Shekouhy, J. Ameri-Rad, *Green Chem.* **13**, 958 (2011)
22. M.B. Gawande, R.V. Jayaram, *Catal. Commun.* **7**, 931 (2006)
23. S. Rana, S. Maddila, K. Yalagala, S.B. Jonnalagadda, *Chem. Pub. Soc.* **4**, 703 (2015)
24. M.J. Aliaga, D.J. Ramon, M. Yus, *Org. Biomol. Chem.* **8**, 43 (2010)
25. D.J. Ramon, M. Yus, *Angew. Chem. Int. Ed.* **44**, 1602 (2005)
26. P.P. Ghosh, A.R. Das, *Tetrahedron Lett.* **53**(25), 3140 (2012)
27. S. Knapp, *Chem. Rev.* **95**, 1859 (1995)
28. D. Seebach, J.L. Matthews, *Chem. Commun.* **21**, 2015(1997)
29. I. Szatmar, F. Fluop, *Curr. Org. Synth.* **1**, 155 (2004)
30. A.Y. Shen, C.T. Tsai, C.L. Chen, *Eur. J. Med. Chem.* **34**, 877 (1999)
31. N.P. Selvam, P.T. Perumal, *Tetrahedron Lett.* **47**, 7481 (2006)
32. B. Das, B. Ravikanth, R. Rao, *J. Mol. Catal. A: Chem.* **261**, 180 (2007)
33. Q. Zhang, J. Luo, Y. Wei, *Green Chem.* **12**, 2246 (2010)
34. R.K. Singh, R. Bala, S. Kumar, *Indian J Chem. B.* **55**, 381 (2016)
35. A.R. Hajipour, Y. Ghayeb, A.E. Ruoho, *Tetrahedron Lett.* **50**, 7220 (2009)
36. K.C. Ashalu, J.N. Rao, *J. Chem. Pharm. Res.* **5**(2), 44–47 (2013)
37. S. Kantevari, L. Nagarapu, *Catal. Commun.* **8**, 1857 (2007)
38. G.H. Mahdavinia, M.A. Bigdeli, M.M. Heravi, *Chin. Chem. Lett.* **19**, 1171 (2008)
39. L. Nagarapu, M. Baseeruddin, S. Apuri, S. Kantevari, *Catal. Commun.* **8**, 1729 (2007)
40. S.N. Shelke, S.R. Bankar, M.B. Gawande, *ACS Sustain. Chem. Eng.* **2**, 1699 (2014)
41. M.B. Gawande, V.D.B. Bonifacio, R.S. Varma, I.D. Nogueira, N. Bundaleski, C.A.A. Ghumman, O.M.N.D. Teodoro, P.S. Branco, *Green Chem.* **15**, 1226 (2013)
42. M.B. Gawande, A.K. Rathi, I.D. Nogueira, R.S. Varma, P.S. Branco, *Green Chem.* **15**(7), 1895 (2013)
43. T. Weber, J.C. Muijsers, J.W. Niemantsverdriet, *J. Phys. Chem.* **100**, 14144 (1996)
44. D.O. Scanlon, G.W. Watson, D.J. Payne, G.R. Atkinson, R.G. Egdell, D.S. Law, *J. Phys. Chem. C* **114**, 4636 (2010)
45. H.M. Lu, W.T. Zheng, Q. Jiang, *J. Phys. D Appl. Phys.* **40**, 320 (2007)
46. M.A. Zolfigol, A. Khazaei, A. Zare, V. Khakyzadeh, *Appl. Catal. A: Gen.* **400**, 70 (2011)
47. A.R. Supale, G.S. Gokavi, *J. Chem. Sci.* **122**(2), 189 (2010)
48. A. Khazaei, M.A. Zolfigol, A.R. Zare, A. Parhami, A. Nezhad, *Appl. Catal. A Gen.* **386**, 179 (2010)
49. M.M. Khodaei, A.R. Khosropour, H. Moghanian, *Synlett* **6**, 916 (2006)
50. H. Moghanian, A. Mobinikhaledi, A.G. Blackman, E. Sarough-Farahani, *RSC Adv.* **4**, 28176 (2014)
51. Z. Nasresfahani, M.Z. Kassae, E. Eidi, *New J. Chem.* **40**, 4720 (2016)